

A Conceptual Design of a Self-Centering Centre Plate

Jose A. Romero-Navarrete, Frank Otremba, Gerardo Hurtado-Hurtado

Abstract—Turning maneuvers originate higher forces exerted on the rail and the loss of locomotive energy, at a rate that is function of several parameters that influence the magnitude of the developed horizontal wheel-rail forces, including the friction at the centre plate and the bogie's yaw stiffness. However, such a friction at the contact surfaces of the centre plate is needed to mitigate the hunting phenomenon when the train moves on straight track segments. In this paper, a self-centering centre plate is proposed, consisting of a lubricated centre plate, equipped with a spring- and damper-based self-centering mechanism. Simulation results of the proposed mechanism suggest that the energy performance in turns of a train car equipped with such self-centering centre plate is comparatively better, as the peak friction forces linked to the dry friction at the contact surfaces of current centre plate designs, are avoided. The assessment of the hunting performance of the proposed device in straight track segments is proposed as the continuation of this work.

Keywords—Bogie's yaw stiffness, bogie's yaw friction, centre plate, self-centering mechanism, turning.

I. INTRODUCTION

RAILWAY safety depends on a variety of factors that include the design characteristics and operational conditions of both, the railway vehicles and infrastructure [1]. In this context, the rail breakage has been identified as a critical situation leading to the whole degradation of the tracks [2] and to the occurrence of derailments [3]. Amongst the different types of railway accidents, derailments can signify catastrophic situations when the spilling of hazardous materials is involved [4], [5]. The failure of the rail material has been associated to such type of railway mishaps [6], [7], as the result of the accumulated effect of vehicle's dynamic loads associated to the steering response of the railway vehicles [8], [9]. The fatigue wear and the performance of the centre plate have been studied from different perspectives. The fatigue wear of this component has been reported by [10], pointing out that such a phenomenon is un-avoidable as the friction at the centre plate is needed, as it contributes to mitigate the bogie hunting vibration phenomena.

Friction at the centre plate also contributes to a transport annoyance: noise [11]. Based upon a simulation approach, the effect of having a lubricated centre plate has been reported as beneficial for reducing the fatigue wear of the rail, but it is recognized that such lubrication promotes the hunting instability of the wheelsets [12]. However, it has been reported

that such friction at the centre plate becomes a secondary influential factor for the rail fatigue wear when compared with the effect of having the rails lubricated to diminish the rail fatigue wear [12]. An intermediate friction level at the centre plate has thus been recommended, to moderate both the rail fatigue wear in turns, and the hunting vibration of the wheelsets in straight railway segments [12]. To cope with this dual situation concerning the effect of the friction at the centre plate, a locking mechanism has been proposed for the center plate [13], in such a way that there is small friction when the vehicle is turning while there is a restraining torque when the vehicle travels along tangents. In this respect, and to the knowledge of the authors, no anti-friction bearings for the centre plate have been implemented, probably because of the larger contact forces at this joint.

Having a rolling-bearing centre plate could thus imply a positive impact for the wearing of the rails in curves, but negatively affect the lateral stability of the railway car. In this context, preliminary outputs from tests assessing the effects of the friction at the centre plate suggest that such a turning resistance has a significant effect on the energy that is lost during turning. Fig. 1 illustrates a schematic representation of the vehicle used in these tests, which is equipped with two different centre plate designs. On the left end of the vehicle, the centre plate includes a spring-acted design which allows changing the normal force at the centre plate, while on the right end, a free rotating centre plate is described. With this design, different levels of spring force are obtained through the turns of the adjusting nut. The vehicle was tested with one centre plate design or with the other, when displacing along a "U turn" track supported on a tilt table, as shown in Fig. 2. The equipment purpose consisted in measuring the loss of potential energy due to the centre plate friction in turns, represented such a loss by the difference in heights from the vehicle initial to its final position (h_i and h_f , respectively). Some preliminary tests were carried out with this equipment, for different levels of spring force (6 adjusting nut positions), for different levels of initial potential energy (small, medium and large).

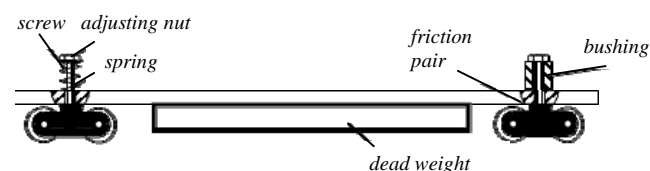


Fig. 1 Schematic representation of a testing car to assess the effect of the friction at the centre plate on the loss of locomotive energy during turning

J. A. Romero-Navarrete is with the Federal Institute for Materials Research and Testing (BAM), Berlin, Germany (corresponding author, phone: +49-30-8104-3919; e-mail: jose-antonio.romero-navarrete@bam.de).

F. Otremba is with the Federal Institute for Materials Research and Testing (BAM), Berlin, Germany (e-mail: frank.otremba@bam.de).

G. Hurtado-Hurtado is a PhD student at the Queretaro Autonomous University, San Juan del Río Campus, México (e-mail: sssp_333@hotmail.com).

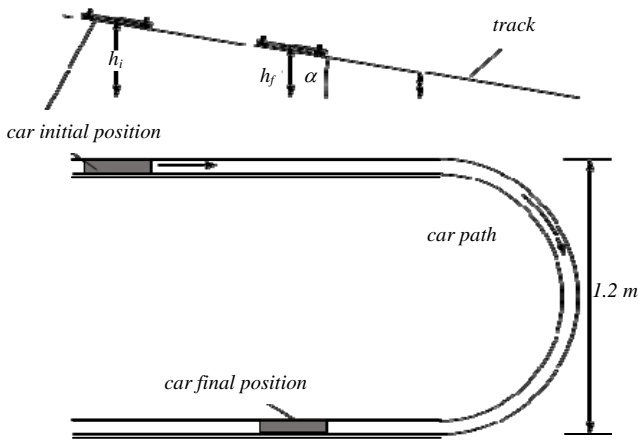


Fig. 2 Experimental principles for assessing the effect of the friction the centre plate on the loss of energy during turning

Fig. 3 illustrates some testing outputs of the lost energy due to turning, for the maximum initial height of the vehicle

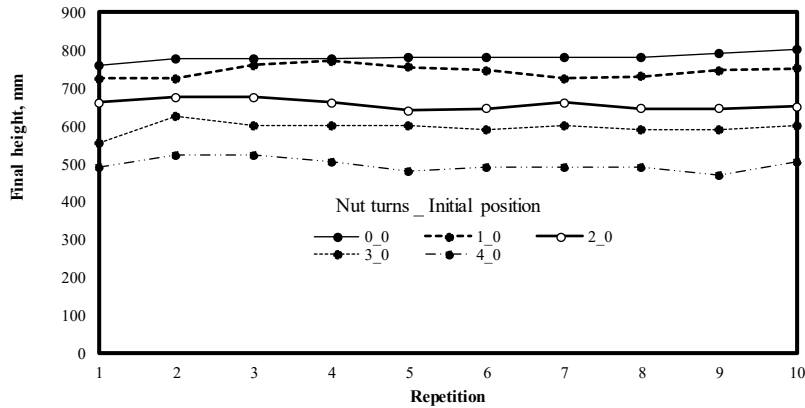


Fig. 3 Experimental outputs for different repetitions, for different number of turns in the adjusting nut

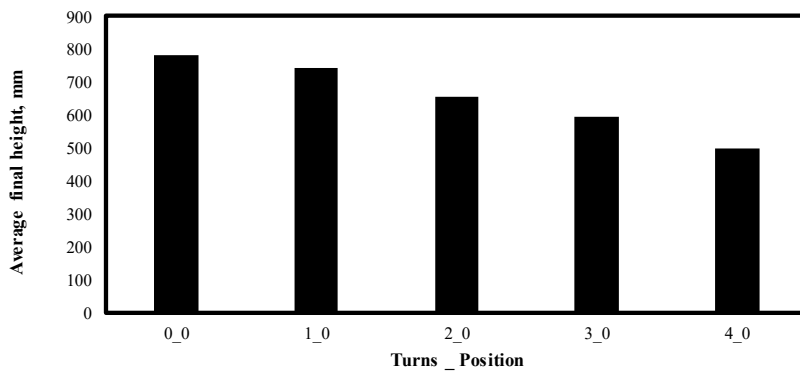


Fig. 4 Average values for the performance measure, for initial position 0 and 5 different turns at the adjusting nut.

(position 0). These results suggest that there is a significant effect of the friction at the centre plate on the magnitude of the lost potential energy. Fig. 4 illustrates the average outputs for the performance measure, as a function of the number of the nut turns, for the initial “position 0” of the vehicle. Fig. 5 illustrates the normalized values of the average outputs, which reveal the importance of the friction at the centre plate. From these data, it results that the sensitivity of the energy loss due to the increase of the normal force and consequent friction force, is about 9% variation in the performance measure, per unit variation in the normal force. Consequently, reducing the friction at the centre plate seems to be a good way to improve the energy efficiency of this type of transportation devices.

In this paper, a design for the centre plate is proposed, whose operation aims at centering the bogie-car relative position in straight segments, while reducing the yaw moment in turns. The overall effect of such a design is considered, focusing in the steering forces developed as a function of the friction and the centering device stiffness.

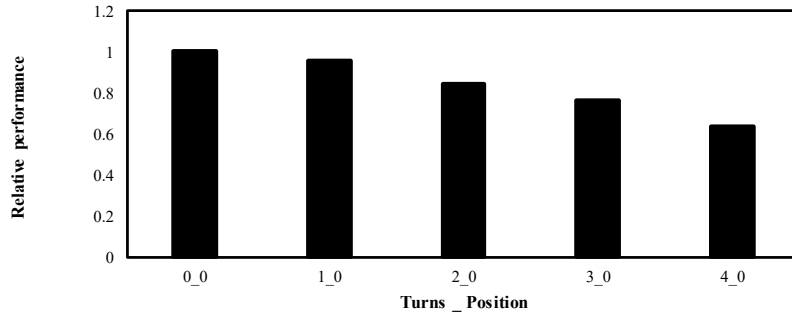
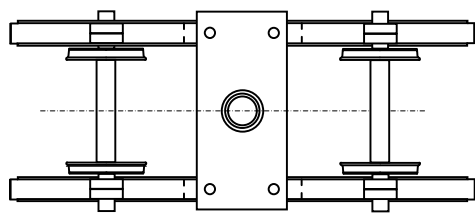


Fig. 5 Normalized values for the performance measure, for initial position 0 and 5 different turns at the adjusting nut.

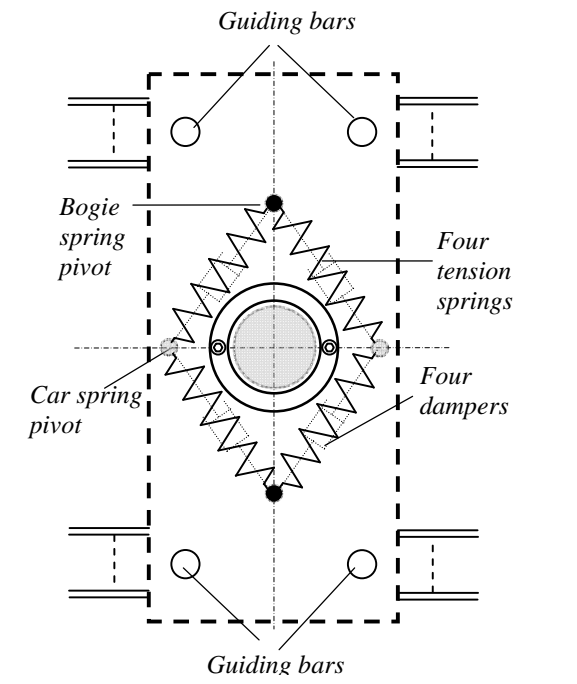
II. SELF-CENTERING MECHANISM CONCEPTUAL DESIGN

A potential improved design for the centre plate might be conceptualized, aiming at mitigating the rail damage potentials of the trains, further contributing to reduce the mobility energy lost during turning maneuvers. For that purpose, the centre plate should provide a minimum friction torque during turnings, while increasing the resistance of the bogie to rotate with respect to the railway car during straight track segments, to moderate the hunting vibration. In this respect, it can be considered a sort of locking mechanism for the bogie orientation with respect to the car. One of such mechanisms, a kind of cam mechanism combined with an antifriction thrust bearing, was proposed in [13]. However, providing a locking mechanism through a cam involves the development of the concentrated fatigue wear of the contact surfaces. Consequently, a mechanism not involving any concentrated friction could be considered, in such a way that the centering force is flexible, further avoiding a concentrated fatigue wear of any contact surfaces of the centre plate. Therefore, the centering force should derive from the action of flexible components that elastically keep the bogie aligned with the railway car longitudinal axis.

Fig. 6 illustrates a potential configuration for a spring-acted centering device. It consists of four tension springs symmetrically arranged around the centre plate. In this figure, the shaded areas correspond to the railway car, and the unshaded ones are bogie's parts. The centre plate contact areas are intended to be fully lubricated, thus representing a minimum friction yaw resistance. This design thus provides an additional yaw stiffness to the bogie, as the secondary suspension represents the main yaw stiffness source. However, it should be noted that the disposition of the added set of springs, is intended to exert a pure rotation resistance torque at the centre plate, in contrast with what the vertical springs of the secondary suspension provide to the bogie-car assembly.



(a) Bogie without spring arrangement



(b) Self centering arrangement

Fig. 6 Spring-acted self-centering mechanism

A sample calculation for the resulting rotational stiffness is presented, for a scaled down mechanism illustrated in Fig. 7, considering a five-degree bogie-car relative rotation. The resultant b and c dimensions are 18.4 mm and 20.1 mm, respectively. The resultant torque is thus expressed as:

$$T = k(\delta_i - 1,8)(20,1) + k(\delta_i + 1,8)(18,4) \quad (1)$$

where d_i is the initial elongation given to the spring. A commercial spring is considered, having an external diameter of 11 mm; a wire diameter of 1.1 mm; and an initial length of 35 mm; and 20 turns. The initial elongation given results as 5.7 mm (40.7 mm – 35 mm). The elongation thus represents a 15% of the initial closed spring length. The measured spring constant for such a spring results as 550 N/m. The torque for each side of the centre plate thus results as:

$$T = .55((5.7 - 1,8)(20,1) + (5.7 + 1,8)(18,4)) = 119 \text{ Nmm} \quad (2)$$

For both sides of the centre plate, the resultant torque is 238 N mm, in such a way that the yaw stiffness results as 2728 N mm /rad.

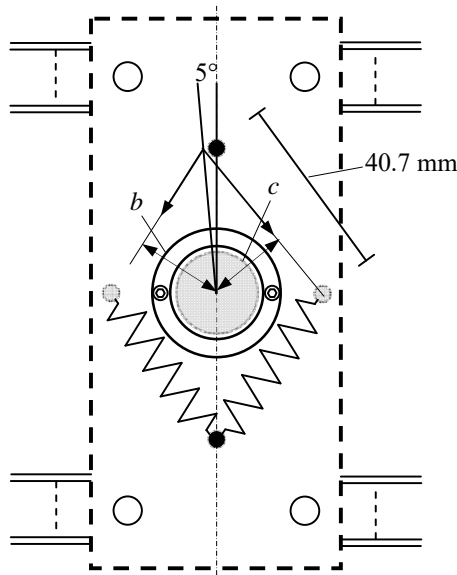


Fig. 7 Resultant forces on one side of the centre plate

The resultant proportions are now scaled up to a full-scale situation, i.e., a 20 times larger arrangement, under the terms of (1). For that purpose, it should be considered that the spring constant k depends on the dimensional and physical characteristics of the spring as [14]:

$$k = \frac{d^4 G}{8D^3 N} \quad (3)$$

where d is the spring wire diameter; D is the spring average diameter, G is the shear modulus; and N is the number of turns. Assuming similar proportional dimensions in order to fill the available space in the centre plate, that is, an external diameter of 100 mm and a wire diameter about 25 mm, for the same number of spring turns (15), the initial length of the spring would be around 656 mm, while the distance between pivots (Fig. 7), would be 814 mm, for an initial elongation of 158 mm. Using (3), the resultant spring constant k is 155000 N/m, and the moment on one side of the centre plate, results as 670727 N mm, or 670.727 N m, totaling 1341 N m on both sides of the centre plate. The yaw stiffness thus results as 15374 N m/rad, when recalling the 5-degree displacement considered in Fig. 7. It should be noted that this resultant yaw stiffness is only a fraction of the standard yaw stiffness of standard centre plate designs (245577 Nm/rad) [15]. These data will be considered in the simulations reported below.

III. MODELLING

For the simulation of the vehicle travelling along a curved track of different radiuses, it is necessary to obtain the steering angle as a function of the geometry of the vehicle and the infrastructure. Fig. 8 illustrates the different characteristics of

the track and the vehicle, when the vehicle is entering the curve and when it is on the curve. The following relationships are obtained:

$$WB \cos(\theta) + r \cos(\gamma) = r \quad (4)$$

$$WB \cos(\pi - \alpha - \gamma) + r \cos(\gamma) = r \quad (5)$$

$$\frac{R}{\sin(\theta)} = \frac{WB}{\sin(\gamma)}; \quad \frac{R}{\sin(\pi - \alpha - \gamma)} = \frac{WB}{\sin(\gamma)} \quad (6)$$

The steering angle ϕ is thus given by:

$$\phi = (\pi / 2) - \alpha \quad (7)$$

These set of equations are solved numerically.

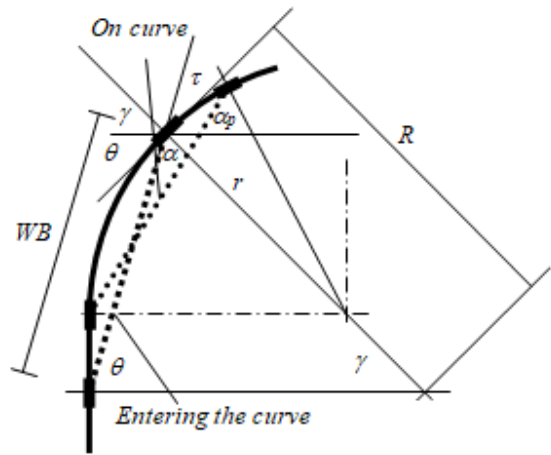


Fig. 8 Geometrical description of a railway car entering and on a curved track segment of radius r

Fig. 9 illustrates the simplified physical model to be used to assess the effect of the yaw stiffness provided the self-centering spring mechanism. This model describes the yaw plane dynamics of the railway car, where no dry friction is considered at the centre plate, while the viscous yaw damping at the centre plate is intrinsic in the device and it is not illustrated in this figure. Such yaw damping will be considered as a factor which will represent different behaviors, including a high-damping situation and a moderate-damping situation. The high damping situation will represent the current design of these devices, while the low-friction situation will describe the centre plate design proposed herein. On the other hand, according to this model, the rear bogie-centre-plate assembly provides a lateral flexibility and damping to the oscillation of the railway car longitudinal chassis, under the assumption of compression springs. Such stiffness is associated to the cross deformation of the rear bogie's secondary suspension. The existing friction and stiffness at the front centre plate will develop lateral forces at the rear centre plate, and the larger magnitudes of such forces will translate into higher damaging effects of the railway car on the rails.

The equation of motion for this system is expressed as a first order system, as:

$$\begin{Bmatrix} \dot{\psi} \\ \dot{\psi} \end{Bmatrix} = \begin{bmatrix} 0 & 1 \\ -\left(\frac{K+kL}{I}\right) & -\left(\frac{C+cL}{I}\right) \end{bmatrix} \begin{Bmatrix} \psi \\ \dot{\psi} \end{Bmatrix} + \begin{bmatrix} 0 & 0 \\ 0 & \left(\frac{K}{I}\right) \end{bmatrix} \begin{Bmatrix} 0 \\ \phi \end{Bmatrix} \quad (8)$$

The selected performance measure is based upon the magnitude of the forces developed at the wheel-rail interface, as a function of the yaw moment, as follows (Fig. 9):

$$F_T = M_T / (4s) \quad (9)$$

$$M_T = K\psi + C\dot{\psi} \quad (10)$$

where s is the arm of the force (Fig. 9).

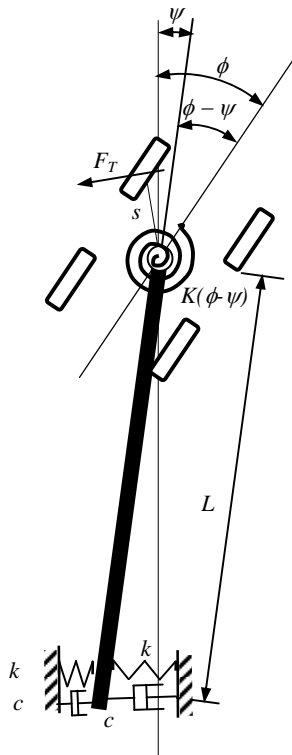


Fig. 9 Simplified one degree-of-freedom physical model for the yaw response of the car

The standard deviation of this force is assumed to be related with the rail damage potentials of the vehicle. The equations of motion (5) are solved through the State Transition Matrix Approach [16]: Four simulations are described of the vehicle traveling along a known path, at different speeds and with different levels of viscous damping at the centre plate, where the yaw stiffness of the secondary front bogie suspension will be incremented due to the spring-acted bogie centering device. Table I illustrates the parameters for the simulations.

The following conditions will be considered in these simulations:

1. Nominal (no self-centering device) yaw stiffness plus high viscous damping. This condition represents the current centre plate design.
2. Nominal (no self-centering device) plus self-centering stiffness, with moderate and null rotational damping at the centre plate. This condition represents the use of the self-centering device, with lubricated centre plate.

According with this approach, the second condition represents the substitution of the dry friction condition at the centre plate, for the stiffness associated to the self-centering device.

Fig. 10 illustrates the path that will be traveled by the simulated vehicle, consisting of a track segment containing three different radiuses, involving two right and one left turns.

TABLE I
 SIMULATION TESTING CONDITIONS

Quantity	Value
K_n , bogie nominal stiffness, Nm/rad [15]	245577
K_s , self-centering device stiffness, Nm/rad	15374
C , bogie viscous damping, N m s /rad	21000
k , car lateral stiffness, N/m	100000
c , car lateral damping	0
Distance between centre plates in a car, m	8
I , railway car mass moment of inertia, kg m ²	200000

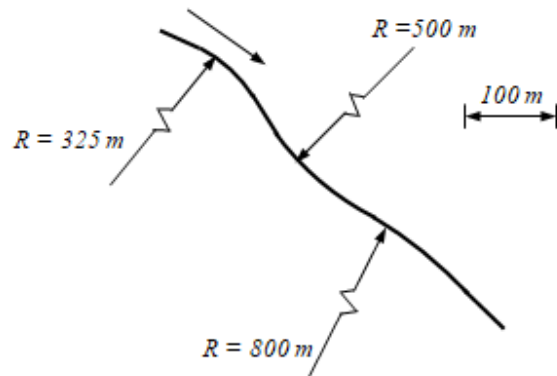


Fig. 10 Track horizontal design

Fig. 11 illustrates the free response of the mechanical system to an initial angular velocity condition, for a moderate damping and non-centering device. Fig. 12 contains the time responses for different conditions. According to the information, there is a small effect of the different situations, with the extreme situations being illustrated by the non-device – high damping; and with device and no-friction. The standard deviation of these time histories is presented in Fig. 13. As it can be observed in this figure, there is a moderate effect of the different conditions, except when the damping is removed.

While the effects are observed as ranging from a small to a moderate level, it should be noted that under real conditions, the dry friction would be generating secondary effects, associated to the stick-slip phenomenon. That is, having a combination of lubrication plus the additional centering stiffness could finally represent a positive effect on the whole dynamics of the vehicle-rail interaction, instead of having a

dry friction centre plate. The lost energy in turning would be decreased by eliminating the stick-slip phenomenon

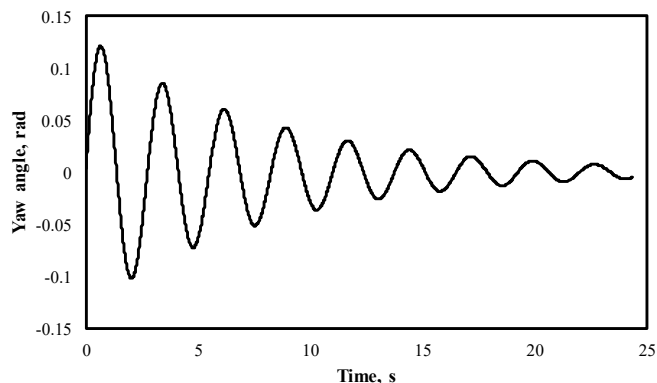


Fig. 11 Yaw free response, without centering device, normal damping

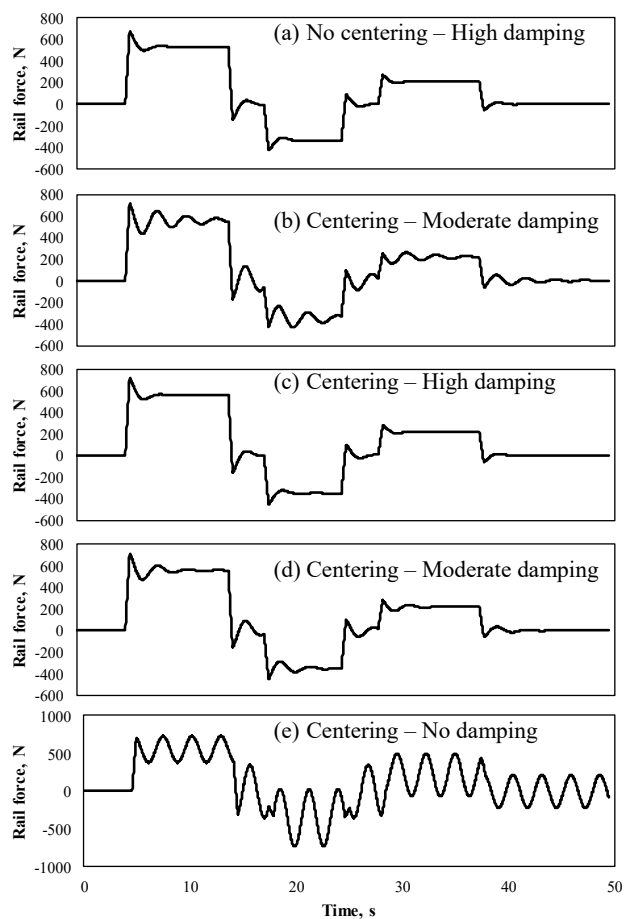


Fig. 12 Time histories for different conditions: with or without the centering device, and with different levels of damping: High damping: 400000 Ns/m; Intermediate damping: 200000 Ns/m; and Moderate damping: 100000 Ns/m

IV. CONCLUSION

When the railway car enters a curve, the vehicle develops steering forces whose magnitude depends on the yaw stiffness of the bogie and on the friction at centre plate. A high friction

at the centre plate is necessary to mitigate the hunting vibration. However, a spring-acted bogie-car centering device could force the alignment of the two bodies, further moderating the hunting vibration. However, increasing the yaw stiffness through such centering device, could further affect the magnitude of the steering forces. In this paper, it has been described the performance of a spring-acted centering device that combined with a moderate friction resistance, would potentially improve the performance of the vehicle while turning, since the lubricated surfaces providing such moderate friction, avoid the force peaks associated to the stick-slip phenomena of the current centre plate designs. The performance of this device under straight track conditions should now be considered.

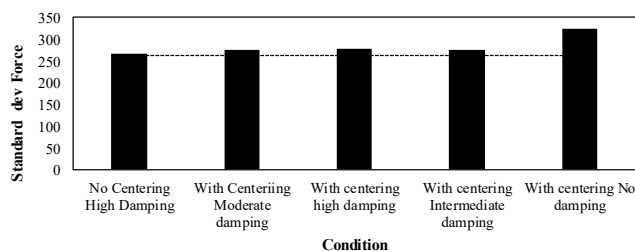


Fig. 13 Standard deviation of the forces, under different testing conditions

REFERENCES

- [1] Grassie, S.L. (2014) Traction, curving and Surface damage or rails, Part 2: Rail damage, Proc. IMechE. Part F: J Rail and Rapid Transit 229(3): 330-339.
- [2] J. N. Varandas, P. Hölscher, M. AG Silva, "Settlement of ballasted track under traffic loading: Application to transition zones", Proceedings of the Institution of Mechanical Engineers, Part F: Journal of Rail and Rapid Transit 228: 242-259, 2014.
- [3] NTSB, "Derailment of Canadian National Freight Train M33371 and Subsequent Release of Hazardous Materials in Tamaroa, Illinois February 9, 2003", Railroad accident report NTSB/RAR-05/01, NTSB, Washington, D.C., 2005.
- [4] Hosseini, S.D., and Verma, M. (2017) A value-at-risk (VAR) approach to routing rail hazmat shipments, Transportation Research Part D 54: 191-211.
- [5] Zakar, F. and Mueller, E. (2016) Investigation of a Columbus, Ohio train derailment caused by fractured rail, Case studies in Engineering Failure Analysis 7: 41-49.
- [6] Liu, X., Saat, M.R., Barkan, Ch. P.L. (2017) Freight-train derailment rates for railroad safety and risk analysis, Accident Analysis and Prevention 98:1-9.
- [7] Magel, E., Mutton, P., Ekberg, A., and Kapoor, A. (2016) Rolling contact fatigue, wear and broken rail derailments, Wear 366-367: 249-257.
- [8] Wang, W.J., Guo, J., Liu, Q.Y., Zhu, M.H., and Zhou, Z.R. (2009) Study on relationship between oblique fatigue crack and rail wear in curve track and prevention, Wear 267: 540-544.
- [9] Schöne, D., Bork, C.-P. (2010) Fatigue investigations of damaged railway rails of UIC 60 profile, Proceedings, 18th European Conference on Fracture: Fracture of Materials and Structures from Micro to Macro Scale, 8p.
- [10] Olshevskiy, A., Kim, Ch-W., Yang, H-I, Olshevskiy, A., Wear simulation for the centre plate arrangement of a freight car. Vehicle System Dynamics 53(6), 856-876 (2015).
- [11] C.E. Tickell, P. Downing, and C.J. Jacobsen, C.J., Rail wheel squeal – some causes and a case study of freight-car wheel squeal reduction, Proceedings of Acoustics 2004, 3-5 November, Gold Cost, Australia. Pp 239-244.
- [12] H. Wu and J. Robeda, Effects of bogie centre plate lubrication on vehicle curving and lateral stability, Vehicle System Dynamics

Supplement 42 (2004), pp 292-301.

- [13] J. A. Romero Navarrete, F. Otremba, A variable friction centre plate. In: Uhl T. (eds) *Advances in Mechanism and Machine Science*. IFToMM WC 2019. *Mechanisms and Machine Science*, vol 73. Springer, Cham.
- [14] Juvinall, R.C., and Marshek, K.M. (2012) *Fundamentals of Machine Component Design*, 5th edition, John Wiley and Sons, Inc. N.J. 929 pp.
- [15] Aizpun, M., Alonso, A., and Vinolas, J. (2016) A new parameter identification methodology for the bogie rotational resistance test of a rail vehicle. *Proc. IMechE Part F: J Rail and Rapid Transit* 230(3), 879-890.
- [16] Meirovitch, L. (1986) *Fundamentals of vibrations*. McGraw-Hill, International Edition, 826 pp.